

Topological aspect of graphene physics

Y. Hatsugai

Institute of Physics, University of Tsukuba, Tsukuba, 305-8571 Japan

E-mail: y.hatsugai@gmail.com

Abstract. Topological aspects of graphene are reviewed focusing on the massless Dirac fermions with/without magnetic field. Doubled Dirac cones of graphene are topologically protected by the chiral symmetry. The quantum Hall effect of the graphene is described by the Berry connection of a manybody state by the filled Landau levels which naturally possesses non-Abelian gauge structures. A generic principle of the topologically non trivial states as the bulk-edge correspondence is applied for graphene with/without magnetic field and explain some of the characteristic boundary phenomena of graphene. ¹

1. Introduction

Graphene as a playground of massless Dirac fermions has a long history of theoretical study[1, 2, 3]. However its experimental realization is a real surprise since the massless Dirac fermion itself is topologically non trivial especially under a magnetic field[4, 5]. It implies that we have a chance to observe exotic topological phenomena in a real world, which have been confirmed experimentally for the past few years.

The quantized Hall conductance is one of the most well-known topological objects as the Chern numbers of the Berry connection which describes the bulk (without boundaries). It is also described by the edge states, supplemented by the Laughlin argument, which gives a different topological number. These two topological quantities are closely related as the bulk-edge correspondence[6]. This bulk-edge relation has been realized as a universal feature of topological states in several different quantum systems such as superconductors, quantum (spin) Hall effects[7, 8, 9], gapped quantum magnets and photonic crystals[10]. The edge states in a magnetic field are chiral fermions in a sense, they have specific direction, and can not be destroyed as far as the bulk is gapped. It is the topological stability of the edge states. Graphene under a magnetic field is one of the typical topological states where the bulk-edge correspondence of the Dirac fermions plays a fundamental role. Localized zero modes near the zigzag boundaries (Fujita states)[11], which have been measured by the STM experiments[12], and their generalization under a magnetic field, are also governed by this topological principle[6]. Further appearance of two Dirac fermions with opposite chirality at the K and K' points are not accidental but is topologically protected by the chiral symmetry which is a two dimensional analogue of the Nielsen-Ninomiya theorem in four dimensions[13].

Also the Landau level of graphene is quite special reflecting its singular dispersion as of the Dirac fermions. Then the quantum Hall effects of it is anomalous[14, 15, 16]. Further Landau degeneracy of the characteristic zero energy Landau level are topologically protected against for

¹ Version:Aug.25 (2010)

some class of randomness by the index theorem. It is fundamental for free-standing single layer graphene where its intrinsic disorder is a gauge field fluctuation[17, 18].

Based on our works, these topological phenomena in graphene physics will be explained intuitively.

2. Topological stability of the Dirac cones and the $n = 0$ Landau level

2.1. Chiral symmetry and doubled Dirac cones

Let us consider a single orbital tight-binding hamiltonian of graphene with magnetic field[16] ($\mathbf{j} = (j_1, j_2)$) is a two dimensional coordinate with the unit translations $\mathbf{e}_{1,2}$ and ϕ is a total flux per hexagon in flux quantum $\Phi_0 = h/e$, See Fig.1)

$$\begin{aligned} H &= t \sum_{\mathbf{j}} \left[c_{\bullet}^{\dagger}(\mathbf{j})c_{\circ}(\mathbf{j}) + e^{2\pi\phi j_1} c_{\bullet}^{\dagger}(\mathbf{j})c_{\circ}(\mathbf{j} - \mathbf{e}_2) + c_{\bullet}^{\dagger}(\mathbf{j} + \mathbf{e}_1)c_{\circ}(\mathbf{j}) + h.c. \right] \quad (\text{zigzag}) \\ &= t \sum_{\mathbf{j}} \left[c_{\bullet}^{\dagger}(\mathbf{j})c_{\circ}(\mathbf{j}) + e^{2\pi\phi(j_1+1)} c_{\bullet}^{\dagger}(\mathbf{j})c_{\circ}(\mathbf{j} + \mathbf{e}_1 - \mathbf{e}_2) + c_{\bullet}^{\dagger}(\mathbf{j} - \mathbf{e}_1)c_{\circ}(\mathbf{j}) + h.c. \right] \quad (\text{bearded}) \end{aligned}$$

where we give two expressions using two different unit cells that are compatible for zigzag and bearded edges. When $\phi = 0$, it is written in the momentum representation as $H = \int \frac{d^2k}{(2\pi)^2} \mathbf{c}^{\dagger}(\mathbf{k}) \mathbf{h}(\mathbf{k}) \mathbf{c}(\mathbf{k})$,

$$\mathbf{h}_{Z,B}(\mathbf{k}) = \begin{pmatrix} 0 & \Delta_{Z,B}(\mathbf{k}) \\ \Delta_{Z,B}^*(\mathbf{k}) & 0 \end{pmatrix}, \quad \begin{cases} \Delta_Z(\mathbf{k}) = t(1 + e^{-ik_1} + e^{-ik_2}) & : (\text{zigzag}) \\ \Delta_B(\mathbf{k}) = t(1 + e^{i(k_1-k_2)} + e^{ik_1}) & : (\text{bearded}) \end{cases}$$

where $\mathbf{c}^{\dagger}(\mathbf{k}) = (c_{\circ}^{\dagger}(\mathbf{k}), c_{\bullet}^{\dagger}(\mathbf{k}))$, $c_{\alpha}(\mathbf{j}) = \int \frac{d^2k}{(2\pi)^2} e^{i\mathbf{k}\cdot\mathbf{j}} c_{\alpha}(\mathbf{k})$. The energy dispersion is given as $\epsilon(\mathbf{k}) = \pm|\Delta(\mathbf{k})|$ and vanishing momenta \mathbf{k}_D , $\Delta(\mathbf{k}_D) = 0$ give massless Dirac cones if exist.

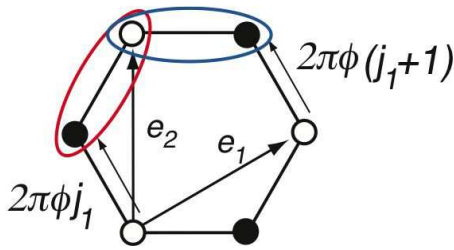


Figure 1. The unit cell of the graphene. The red ellipse is consistent with the zigzag edges and the blue one is for the bearded one. Two primitive translation vectors are also shown.

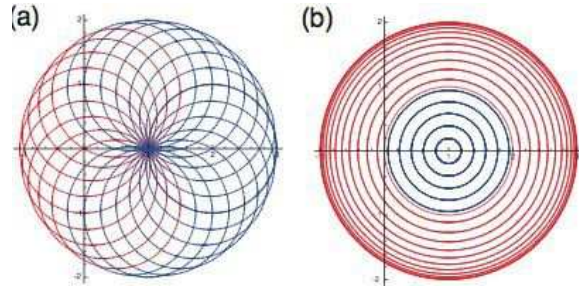


Figure 2. Trajectories of $\Delta(\mathbf{k})$ parametrized by k_1 for various values of k_2 . (a) for $\Delta = \Delta_Z$ and (b) $\Delta = \Delta_B$ ($t = -1$). Curves that encloses the origin is drawn in red.

Since the Brillouin zone, $T^2 = \{(k_1, k_2) | k_1, k_2 \in [0, 2\pi]\}$, is a two-torus by identifying $k_1 = 0 \Leftrightarrow k_1 = 2\pi$ and $k_2 = 0 \Leftrightarrow k_2 = 2\pi$, it does not have boundaries. Then considering k_1 as a parameter, $\Delta(\mathbf{k})$ makes a closed loop in the complex plane for each fixed k_2 . This loop is modified by changing k_2 from 0 to 2π and comes back to the original one (Fig.2). When the loop cuts the origin, it gives the Dirac cone. Then once the loop cuts the origin, the situation is stable against for small but finite perturbation. This is the topological stability of the Dirac cones. Here we need the 2×2 hamiltonian is characterized by single complex parameter Δ (diagonal

parts are zero). This is the *chiral symmetry*, that is, there exists $\{\mathbf{h}, \gamma\} = 0$, $\gamma^2 = \sigma_0$: 2×2 unit matrix. (In this case, $\gamma = \sigma_3$.) Also the doubling of the Dirac cones is again clear since the origin cutting the loop from the outside to the inside inevitably followed by cutting from inside to the out (See Fig.2 and Fig.4). This simple observation guarantees that the number of Dirac cones are always even. Note here that the chiral symmetry is related to the bipartite structure of the honeycomb lattice, that is, the hoppings are only between the two sub-lattices \circ and \bullet .

On the other hand, as for generic semiconductors including graphene, let us assume the effective hamiltonian of the valence and the conduction bands, \mathbf{h} , is chiral symmetric, that is, it does anti-commutes with some chiral matrix γ , $\{\mathbf{h}, \gamma\} = 0$. It implies \mathbf{h} is traceless and thus one can expand it by the Pauli matrices as $\mathbf{h}(\mathbf{k}) = \mathbf{R}(\mathbf{k}) \cdot \boldsymbol{\sigma}$ with three real parameters $R_1(\mathbf{k})$, $R_2(\mathbf{k})$ and $R_3(\mathbf{k})$ that makes a vector $\mathbf{R}(\mathbf{k}) = \begin{pmatrix} R_1(\mathbf{k}) \\ R_2(\mathbf{k}) \\ R_3(\mathbf{k}) \end{pmatrix}$. The momentum dependent energy gap is $E_g(\mathbf{k}) = 2|\mathbf{R}(\mathbf{k})|$. Then the zero gap condition is $\mathbf{R} = \mathbf{0}$. Writing the chiral matrix as, $\gamma = \mathbf{n}_\gamma \cdot \boldsymbol{\sigma}$ ($\mathbf{n}_\gamma^2 = 1$), the chiral symmetric condition $\{\mathbf{h}, \gamma\} = (\mathbf{R} \cdot \mathbf{n}_\gamma)\sigma_0 + i(\mathbf{R} \times \mathbf{n}_\gamma) \cdot \boldsymbol{\sigma} + (\mathbf{R} \rightrightarrows \mathbf{n}_\gamma) = 2(\mathbf{R} \cdot \mathbf{n}_\gamma)\sigma_0 = 0$, implies $\mathbf{R} \cdot \mathbf{n}_\gamma = 0$, that is, \mathbf{R} is always in the plane $\mathbb{R}^2(\mathbf{n}_\gamma)$ whose normal vector is \mathbf{n}_γ . Since the Brilluine zone T^2 is a 2-dimensional closed surface, the image $\mathbf{R}(T^2)$ is also a closed surface (like a balloon) in 3-dimensions. Then the condition $\mathbf{R}(T^2) \subset \mathbb{R}^2(\mathbf{n}_\gamma)$ means the closed surface is collapsed on the plane (a rubber balloon without air on the desk). When the collapsed image includes the origin, it gives the Dirac cones. Then the topological stability of the Dirac cones and the doubling of them are clear[16, 19, 20]. (See Figs3.) It is the 2-dimensional analogue of the Nielsen-Ninomiya theorem in the 4-dimensional lattice gauge theory [13]. A relation between the 4D graphene and chiral fermions is recently discussed as well[21].

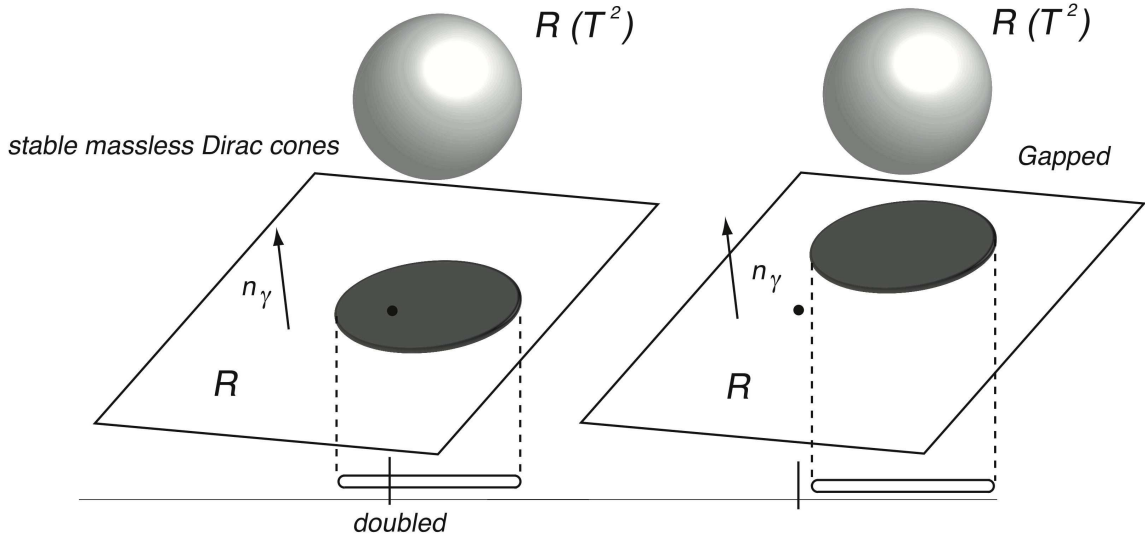


Figure 3. Topological stabilities of the Dirac cones. The image of the Brillouine zone $\mathbf{R}(T^2)$ is generically a surface in three dimensional space \mathbf{R} , which is collapsed into the plane which is normal to the \mathbf{n}_γ , when the hamiltonian is chiral symmetric as $\{H, \gamma\} = 0$, $\gamma = \boldsymbol{\sigma} \cdot \mathbf{n}_\gamma$.

2.2. Chiral symmetry and the $n = 0$ Landau level

Now let us expand the hamiltonian $\mathbf{h}(\mathbf{k})$ with chiral symmetry ($\{\mathbf{h}, \gamma\}$) near one of the doubled zero gap momentum, say, \mathbf{k}_D . Then the effective hamiltonian in the lowest order in $\delta\mathbf{k} = \mathbf{k} - \mathbf{k}_D$ is written as $\mathbf{h} \approx \mathbf{h}_C = \delta k_1 \boldsymbol{\sigma} \cdot \mathbf{X} + \delta k_2 \boldsymbol{\sigma} \cdot \mathbf{Y}$ where $\mathbf{X} = \partial_{k_1} \mathbf{R}$ and $\mathbf{Y} = \partial_{k_2} \mathbf{R}$ which are perpendicular to the \mathbf{n}_γ . It implies the chiral symmetry of the effective hamiltonian, $\{\mathbf{h}_C, \gamma\} = 0$. One may define the chirality of the effective hamiltonian $\chi_D = \pm 1$ as $\mathbf{n}_\gamma = \chi_D \mathbf{X} \times \mathbf{Y} / (c\hbar)^2$ where the effective *light velocity* ($c > 0$) is defined as $c^2 \equiv |\mathbf{X} \times \mathbf{Y}| / \hbar^2$. When the vector, $(\mathbf{X}, \mathbf{Y}, \mathbf{n}_\gamma)$, forms a right handed triple, the chirality, χ_D is +1 and, if left-handed, $\chi_D = -1$. Then the chiral matrix is written as $\gamma = \chi_D \boldsymbol{\sigma} \cdot (\mathbf{X} \times \mathbf{Y}) / (c\hbar)^2$.

By the inverse procedure of the quantization, $\hbar\delta\mathbf{k} \rightarrow \mathbf{p} - e\mathbf{A} \equiv \boldsymbol{\pi}$, $p_\alpha = -i\hbar\partial_\alpha$, ($\alpha = x, y$), we have a real space form of the effective hamiltonian with a magnetic field, $B = \partial_x A_y - \partial_y A_x > 0$, $[\pi_x, \pi_y] = i\hbar eB$ as

$$\mathbf{h}_C = \hbar^{-1} [(\boldsymbol{\sigma} \cdot \mathbf{X})\pi_x + (\boldsymbol{\sigma} \cdot \mathbf{Y})\pi_y]$$

The spectrum and the wave functions are determined by considering its square as

$$\begin{aligned} \mathbf{h}_C^2 &= \hbar^{-2} [\mathbf{X}^2 \pi_x^2 + \mathbf{Y}^2 \pi_y^2 + (\mathbf{X} \cdot \mathbf{Y})(\pi_x \pi_y + \pi_y \pi_x) + i(\mathbf{X} \times \mathbf{Y}) \cdot \boldsymbol{\sigma} [\pi_x, \pi_y]] \\ &= c^2 (\boldsymbol{\pi}^\dagger \Xi \boldsymbol{\pi}) \boldsymbol{\sigma}_0 - \chi_D (eB\hbar c^2) \boldsymbol{\gamma} \end{aligned}$$

where

$$\begin{aligned} \Xi &= \frac{1}{(\hbar c)^2} (\mathbf{X}, \mathbf{Y})^\dagger (\mathbf{X}, \mathbf{Y}) = \frac{1}{(\hbar c)^2} \begin{pmatrix} \mathbf{X} \cdot \mathbf{X} & \mathbf{X} \cdot \mathbf{Y} \\ \mathbf{X} \cdot \mathbf{Y} & \mathbf{Y} \cdot \mathbf{Y} \end{pmatrix} \\ \det \Xi &= \frac{1}{(\hbar c)^4} (|\mathbf{X}|^2 |\mathbf{Y}|^2 - (\mathbf{X} \cdot \mathbf{Y})^2) = \frac{|\mathbf{X} \times \mathbf{Y}|^2}{(\hbar c)^4} = 1 \end{aligned}$$

By identifying as $\frac{1}{2m} \equiv c^2$, the first term of \mathbf{h}_C is considered as a hamiltonian of the standard parabolic electrons with anisotropic masses (See Appendix A). Here the cyclotron frequency ω_C is identified as $\omega_C = eB/m = 2eBc^2$. Also note that the chiral matrix, $\boldsymbol{\gamma}$, commutes with the squared hamiltonian \mathbf{h}_C^2 .

Then writing a normalized standard Landau state with energy, $\hbar\omega_C(n + 1/2) = 2\hbar eBc^2(n + 1/2)$, $n = 0, 1, 2, \dots$, as $\psi_n(x, y)$, the eigen state of \mathbf{h}_C^2 is written as $\boldsymbol{\Psi}_n^\pm = \boldsymbol{\varphi}_\pm \psi_n(x, y)$ where $\boldsymbol{\varphi}_\pm$ is an eigen state of $\boldsymbol{\gamma}$ with eigen values ± 1 respectively. It satisfies $\mathbf{h}_C^2 \boldsymbol{\Psi}_n^\pm = (eB\hbar c^2)(2n + 1 \mp \chi_D) \boldsymbol{\Psi}_n^\pm$. It implies that the effective hamiltonian \mathbf{h}_C always has a zero energy Landau level as

$$\boldsymbol{\Psi}_{\chi_D}^0(x, y) \equiv \boldsymbol{\varphi}_{\chi_D} \psi_0(x, y) \quad : \quad \mathbf{h}_C \boldsymbol{\Psi}_{\chi_D}^0(x, y) = 0$$

which has the chirality χ_D .

As for the non zero energy Landau levels, \mathbf{h}_C^2 is doubly degenerated at ϵ_n^2 , $\epsilon_n = c\sqrt{2neB\hbar}$, spanned by $\boldsymbol{\Psi}_n^{+\chi_D} = \boldsymbol{\varphi}_{+\chi_D} \psi_n(x, y)$ and $\boldsymbol{\Psi}_{n-1}^{-\chi_D} = \boldsymbol{\varphi}_{-\chi_D} \psi_{n-1}(x, y)$, which diagonalize \mathbf{h}_C without degeneracy with the energies $\pm\epsilon_n$.

2.3. Chiral symmetry and Fermion doubling

Up to this point, we have discussed the effective theory of the chiral symmetric zero gap semiconductor near one of the gapless momentum.

As discussed the chiral symmetry of the global hamiltonian \mathbf{h} , $\{\mathbf{h}(\mathbf{k}), \gamma\} = 0$, ($\mathbf{h} = \mathbf{R} \cdot \boldsymbol{\sigma}$) requires that the three dimensional vector $\mathbf{R}(\mathbf{k})$ is always perpendicular to the \mathbf{n}_γ and on the plane $\mathbb{R}^2(\mathbf{n}_\gamma)$ cutting the origin $\mathbf{R} = 0$ ($\mathbf{R}(\mathbf{k}) \in \mathbb{R}^2(\mathbf{n}_\gamma)$). Then one can repeat the discussion for $\Delta(\mathbf{k})$ in Fig.2 for the contour $\mathbf{R}()$ on the plane $\mathbb{R}^2(\mathbf{n}_\gamma)$, that is, considering a closed curve characterized by k_2 , $C(k_2) = \{\mathbf{k} | k_1 \in [0, 2\pi]\}$. This curve is on the plane $\mathbb{R}^2(\mathbf{n}_\gamma)$ and comes back to the original one by changing k_1 form 0 to 2π . When it cuts the origin, it gives the Dirac cones. The doubling of the Dirac cones is also clear as before (Figs.2 and 4). Also as for the chirality of the Dirac cones, χ_D , the paired Dirac cones, D and D' , have a reversed chirality as

$$\chi_D + \chi_{D'} = 0$$

which is also clear from the Fig.4. Then the chirality of the $n = 0$ Landau level is also reversed. As for the graphene, the Dirac fermions at K and K' do have the reversed chirality.

2.4. Aharonov-Casher argument

As discussed the $n = 0$ Landau level is an eigen state of the chiral operator for each Dirac fermion which is a characteristic feature of the chiral symmetric massless Dirac fermions on lattice. It is realized in graphene. This complete degeneracy of the Landau level is not only for the pure system and it does persist for some class on the randomness[?]. There is well-known discussion by Aharonov-Casher[22] which is considered as a direct demonstration of the index theorem where the degeneracy is only determined by the total flux passing through the system as far as the effective description by the Dirac fermions is allowed. Here the magnetic field B may not be uniform. We compactly describe it extending the discussion to our anisotropic case. Since the anisotropic mass matrix Ξ discussed before is real symmetric and its determinant unity, it is diagonalized by the orthogonal matrix \mathbf{V} as (See also appendix), $\Xi = \mathbf{V}^\dagger \begin{pmatrix} \xi_X & \\ & \xi_Y \end{pmatrix} \mathbf{V}$, where $\xi_X, \xi_Y > 0$, $\xi_X \xi_Y = 1$. Then defining canonical momenta $\Pi = \mathbf{V} \boldsymbol{\pi}$, $[\Pi_X, \Pi_Y] = [\pi_x, \pi_y] = i\hbar eB$, \mathbf{h}_C^2 is factorized as

$$\begin{aligned} \mathbf{h}_C^2 &= c^2(\xi_X \Pi_X^2 + \xi_Y \Pi_Y^2) + i\chi_D \gamma [\Pi_X, \Pi_Y] = c^2 \mathcal{D}^\dagger \mathcal{D} \\ \mathcal{D} &= \sqrt{\xi_X} \Pi_X + i\chi_D \gamma \sqrt{\xi_Y} \Pi_Y \end{aligned}$$

Then writing the vector potential as $A_X = -\xi_Y \partial_Y \phi$, $A_Y = \xi_X \partial_X \phi$ and defining $\tilde{X} = X/\sqrt{\xi_X}$ and $\tilde{Y} = Y/\sqrt{\xi_Y}$ ($\sqrt{\xi_X} \partial_X = \partial_{\tilde{X}}$ and $\sqrt{\xi_Y} \partial_Y = \partial_{\tilde{Y}}$), the zero mode $\Psi_{\chi_D}^0 = \varphi_{\chi_D} \psi$ satisfies, $0 = \mathcal{D} \psi_{\chi_D}^0 = -i\hbar \left[\partial_{\tilde{X}} + i\frac{2\pi}{\phi_0} \partial_{\tilde{Y}} \phi + i\partial_{\tilde{Y}} + \frac{2\pi}{\phi_0} \partial_{\tilde{X}} \phi \right] \psi_{\chi_D}^0$. Then writing as $\psi_0 = e^{-2\pi \frac{\phi}{\phi_0}} f$, the function f satisfies $(\partial_{\tilde{X}} + i\partial_{\tilde{Y}})f = 0$. This is written by defining $z = \tilde{X} + i\tilde{Y}$ as $\partial_z f = 0$. Thus the function f is an entire function of z in the whole complex plane $z \in \mathbb{C}$, that is, polynomials. Also note that the function ϕ needs to satisfy $B = \partial_X A_Y - \partial_Y A_X = (\xi_X \partial_X^2 + \xi_Y \partial_Y^2) \phi = (\partial_{\tilde{X}}^2 + \partial_{\tilde{Y}}^2) \phi$. It implies $\phi(\tilde{X}, \tilde{Y}) = \int d\tilde{X} d\tilde{Y} G(\tilde{X} - \tilde{X}', \tilde{Y} - \tilde{Y}') B(\tilde{X}', \tilde{Y}')$ where $G(\tilde{X}, \tilde{Y}) = \frac{1}{2\pi} \log \frac{r}{r_0}$, $r^2 = \tilde{X}^2 + \tilde{Y}^2$ and r_0 is a constant. When assuming the magnetic field is only nonzero in the finite region, we have for the asymptotic behavior in the limit $r \rightarrow \infty$ as $\phi \xrightarrow{r \rightarrow \infty} \frac{\Phi}{2\pi} \log \left(\frac{r}{r_0} \right)$ where $\Phi = \int d\tilde{X} d\tilde{Y} B = \int dX dY B$ is a total flux. Then we have for the asymptotic behavior of the zero mode as $\psi \xrightarrow{r \rightarrow \infty} f(z) \left(\frac{r}{r_0} \right)^{-\frac{\Phi}{\phi_0}}$. It implies that the number of the degeneracy is $\frac{\Phi}{\phi_0}$.

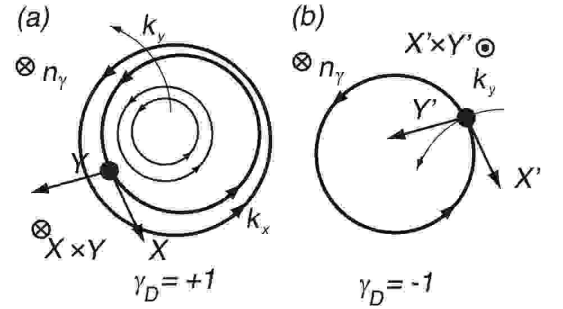


Figure 4. $\mathbf{R}(\mathbf{k})$ on the plane $\mathbb{R}^2(\mathbf{n}_\gamma)$. (a) When the curve cuts the origin which defines the Dirac cone. (b) Another Dirac cone which is paired with the one in (a). The chirality is reversed.

3. Hall conductance and Berry connection of Dirac sea

Geometrical phase of the quantum mechanical states are of fundamental interest for physical society today. The quantum Hall effect and its time reversal invariant analogue as the quantum spin Hall effect are the typical examples.

Now let us start from the Niu-Thouless-Wu formula for the Hall conductance[23]. It reads that the Hall conductance of the manybody state is given by the average over the twisted boundary condition as

$$\sigma_{xy} = \frac{e^2}{h}C, \quad C = \frac{1}{2\pi i} \int_0^{2\pi} d\phi^1 \int_0^{2\pi} d\phi^2 [\langle \partial_1 G | \partial_2 G \rangle - \langle \partial_2 G | \partial_1 G \rangle]$$

where $\partial_\mu = \frac{\partial}{\partial \phi^\mu}$, ($\mu = x, y$) and where $|G\rangle = |G(\phi^1, \phi^2)\rangle$ is a unique gapped ground state of the hamiltonian, $H(\phi^1, \phi^2)$, with a twisted boundary condition specified by $e^{i\phi^1}$ and $e^{i\phi^2}$ for each of the two translational directions as $H|G\rangle = E|G\rangle$.

This C is the topological number (Chern number) and is intrinsically integer as explained below. This topological property is clearly demonstrated by defining the Berry connection (a formal form of the vector potential) as

$$\mathcal{A} = \langle G | dG \rangle = \langle G | \partial_\mu G \rangle d\phi^\mu = d\phi \cdot \mathbf{A}, \quad \mathbf{A} = \langle G | \nabla G \rangle$$

where $\phi = (\phi^1, \phi^2, 0)$ and $\nabla = (\partial_1, \partial_2, \partial_3)$. Note that, since the phase of the state $|G\rangle$ is completely arbitrary, one may take a different choice as $|G'\rangle = |G\rangle\omega$, $\omega = e^{i\theta}$, $\theta \in \mathbb{R}$, which gives a different connection $\mathcal{A}' = \langle G' | dG' \rangle = d\phi \cdot \mathbf{A}'$. They are related with each other as [24]

$$\mathcal{A} = \mathcal{A}' + \omega^{-1}d\omega = \mathcal{A}' + id\theta, \quad \mathbf{A} = \mathbf{A}' + i\nabla\theta$$

This is the gauge transformation similar to the case of the electromagnetic field governed by the Maxwell equations. (As for the differential form, see [25].) This is called Abelian since ω is just a complex number $|\omega| = 1$.

Since the twisted boundary condition of $e^{i2\pi}$ is equivalent to the periodic boundary condition without any twist, the integral region $T^2 = \{(\phi^1, \phi^2) | \phi^\mu \in [0, 2\pi]\}$ is identified as the two-torus. Then the Chern number of the manybody state is written as

$$C = \frac{1}{2\pi i} \int_{T^2} d\mathbf{S} \cdot \text{rot } \mathbf{A} = \frac{1}{2\pi i} \int_{T^2} d\mathcal{A} \equiv \frac{1}{2\pi i} \int_{T^2} \mathcal{F} = \frac{1}{2\pi i} \int_{T^2} \langle dG | dG \rangle$$

where $d\mathbf{S} = d\phi^1 d\phi^2 (0, 0, 1)$ and the field strength is defined as $\mathcal{F} = d\mathcal{A} = \langle dG | dG \rangle$. The connection \mathcal{A} is gauge dependent but the Abelian field strength \mathcal{F} is gauge invariant as $\mathcal{F}' = d\mathcal{A}' = d\mathcal{A}$ since $d(\omega^{-1}d\omega) = -\omega^{-1}d\omega\omega^{-1}\omega = -(\omega^{-1}d\omega)^2 = 0$ (See Appendix B).

To understand the quantization of the Hall conductance, we need to specify the gauge[26]. Here we discuss this gauge fixing generically[27]. Since the two-torus T^2 is boundaryless, the Chern number is always vanishing if one is allowed to use the Stokes theorem globally $C = \int_{T^2} d\mathcal{A} = \int_{\partial T^2 = \emptyset} \mathcal{A} = 0$. To have a nonzero Chern number, the single global gauge is not allowed and one needs to use two different gauges, at least, say, \mathcal{A}_1 and \mathcal{A}_2 . Let us first mention that the state $|G\rangle$ is gauge dependent but the projection into the ground state space $P = |G\rangle\langle G| = |G'\rangle\langle G'|$ is gauge invariant. Then taking arbitrary (fixed) state $|T_1\rangle$, a normalized and gauge fixed state $|G_1\rangle$ is given as $|G_1\rangle = P|T_1\rangle/\sqrt{N_1}$ where $N_1 = \langle T_1 | P | T_1 \rangle =$

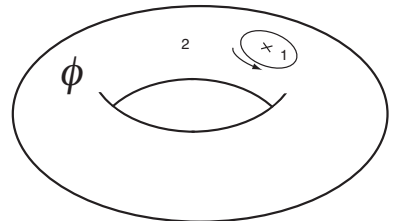


Figure 5. Singularity of the gauge and the two patches to avoid it.

$|\langle G|T_1\rangle|^2 \geq 0$ is a gauge invariant normalization constant. It is clear that this gauge becomes singular when the normalization N_1 is vanishing at some point in T^2 ($N_1 = 0$). Near this singular point ϕ_1 , one needs to use the other gauge, say $|G_2\rangle$ using another arbitrary state $|T_2\rangle$ that is generically regular in the region R_1 that includes ϕ_1 , $N_2(\phi) \neq 0, \phi \in R_1$.

The gauge transformation between the two, $\mathcal{A}_1 = \mathcal{A}_2 + i\theta_{21}$ is given as $|G_1\rangle = |G_2\rangle\omega_{21}$, $\omega_{21} = \langle T_2|P|T_1\rangle/\sqrt{N_1N_2} = e^{i\theta_{21}}$. When these two gauges are enough to span the whole ϕ space, the Chern number is written as

$$C = \frac{1}{2\pi i} \left(\int_{R_1} d\mathcal{A}_2 + \int_{T^2 \setminus R_1} d\mathcal{A}_1 \right) = \frac{1}{2\pi i} \int_{\partial R_1} (\mathcal{A}_1 - \mathcal{A}_2) = \frac{1}{2\pi} \oint_{\partial R_1} d\theta_{21}$$

Here the reason the Chern number is integer is clear since the gauge transformation ω_{21} is single valued on the boundary ∂R_1 .

When the system is non-interacting, $V = 0$, one may go further. In this case, the ground state of the many body system, (M particle state), $|G\rangle$ is constructed from one particle states. It is explicitly expressed by writing the hamiltonian as $H = \mathbf{c}^\dagger(\mathbf{h})\mathbf{c}$ where $\mathbf{c}^\dagger = (c_1, \dots, c_N)$ and N is a total number of system sites. The ground state is given by the filling the one particle states below the fermi energy ϵ_F as ($\epsilon_M \leq \epsilon_F$)

$$|G\rangle = |\Psi\rangle = \prod_{\ell=1}^M \mathbf{c}^\dagger \psi_\ell |0\rangle, \quad \mathbf{h}\psi_\ell = \epsilon_\ell \psi_\ell, \quad \epsilon_\ell \leq \epsilon_{\ell'}, (\ell < \ell'), \quad \psi_\ell^\dagger \psi_{\ell'} = \delta_{\ell\ell'}$$

where the many body state is labeled by the filled one particle state, that form a multiplet, $\Psi = (\psi_1, \dots, \psi_M)$ [28, 29, 30]. The Berry connection of this non-interacting ground state has an interesting form by the non-Abelian Berry connection \mathbf{A}_M which is defined as

$$\begin{aligned} \mathcal{A} &= \langle g | \sum_{\ell} (\mathbf{c}^\dagger \psi_1) \cdots (\mathbf{c}^\dagger d\psi_\ell) \cdots (\mathbf{c}^\dagger \psi_M) | 0 \rangle = \sum_{\ell} \det_M \Psi^\dagger(\psi_1, \dots, d\psi_\ell, \dots, \psi_M) = \text{Tr } \mathbf{A}_M \\ \mathbf{A}_M &= \Psi^\dagger d\Psi = \begin{bmatrix} \psi_1^\dagger d\psi_1 & \psi_1^\dagger d\psi_2 & \cdots \\ \psi_2^\dagger d\psi_1 & \psi_2^\dagger d\psi_2 & \cdots \\ \vdots & \vdots & \ddots \end{bmatrix}. \end{aligned}$$

Here the choice of the one particle states below the fermi energy is arbitrary and one may further allow to mix up among them as

$$\Psi = \Psi' \omega, \quad \omega^\dagger \omega = E_M$$

which results in the same many body state $|\Psi\rangle = |\Psi'\rangle \det \omega$ since $\omega \in U(M)$ and $\det \omega \in U(1)$. This \mathbf{A}_M defines a non-Abelian Berry connection. Its property under the gauge transformation is given as [31, 27]

$$\mathbf{A}_M = \omega^{-1} \mathbf{A}'_M \omega + \omega^{-1} d\omega$$

This is the gauge transformation of the non Abelian matrix valued connection spanned by the filled one particle states. Correspondingly the field strength (matrix) is defined as

$$\mathbf{F}_M \equiv d\mathbf{A}_M + \mathbf{A}_M^2 = \sum_{\mu < \nu} \mathbf{F}_{\mu\nu} d\phi^\mu d\phi^\nu, \quad \mathbf{F}_{\mu\nu} = \partial_\mu \mathbf{A}_\nu - \partial_\nu \mathbf{A}_\mu + [\mathbf{A}_\mu, \mathbf{A}_\nu]$$

It transforms as $\mathbf{F}_M = \boldsymbol{\omega}^{-1} \mathbf{F}'_M \boldsymbol{\omega}$. This non Abelian field strength is directly related to the field strength of the manybody state

$$\mathcal{F} = \text{Tr } \mathbf{F}_M$$

which gives the TKNN formula when each Landau levels are well separated[32]. It transforms as $\mathcal{F} = \text{Tr } \mathbf{F}_M = \mathcal{F}' = \text{Tr } \mathbf{F}'_M$, which is consistent with the physical observable σ_{xy} is independent of the choice of the one particle state.

The advantage of this non-Abelian formulation is that we do not need to sum up all Chern numbers of the filled one particle states. We just need to evaluate the matrix values field strength. This is especially useful for the graphene in a weak magnetic field. Since we are mainly interested in the Hall conductance when the fermi energy is near zero. Then one need to evaluate all Chern numbers of Landau levels with negative one particle states energies (Landau levels of Dirac sea). The final result is expected to be of the order of unity. It implies most of the Chern numbers of the filled Dirac sea are canceled. That is, making one error in evaluating each Chern numbers causes a serious problem on the final results.

Also we mentioned here a numerical technique developed in the lattice gauge theory to evaluate lattice topological invariants are quite useful for the evaluation of the $U(1)$ part of the non Abelian Berry connection, which is a two-dimensional analogue of the King Smith-Vanderbilt formula for the polarization, this is a lattice version of the one-dimensional line integral[33]. This non Abelian method is applied for calculation of the Hall conductance of graphene with realistic multi using non orthogonal bases[34].

4. Bulk edge correspondence

Based on the decades of studies for topological states in condensed matter physics, it has been widely understood that although the bulk of topologically non trivial states is featureless and does not show any fundamental symmetry breaking, near their boundaries and defects as local perturbation, there are characteristic local physics governed by the edge states. This is the *bulk-edge correspondence* that can be useful to investigate topological phases both theoretically and experimentally[6]. As for the graphene, there have been two types of interesting boundary phenomena. One is the boundary states at the zigzag edge with/without magnetic field and the other is quantum Hall edge states of the Dirac fermions. Both of them are fundamentally controlled by the bulk which we demonstrate here.

To investigate, let us put the graphene on the cylinder (Fig.6) with zigzag-bearded edges. Let us then take a momentum representation only in tangential \mathbf{e}_2 direction as $c_\alpha(\mathbf{j}) = \int \frac{dk_2}{d2\pi} e^{ik_2 j_2} c_\alpha(j_1, k_2)$. Now the total hamiltonian is decomposed as $H = \int \frac{dk_2}{d2\pi} H_{cyl}(k_2)$ by a one dimensional hamiltonian $H_{cyl}(k_2)$ with k_2 as a parameter. $H_{cyl} = [t_{\bullet\circ}(j_1) c_{\bullet}^\dagger(j_1+1) c_\circ(j_1) + t_{\circ\bullet}(j_1) c_{\circ}^\dagger(j_1) c_{\bullet}(j_1) + h.c.]$ where $c_\alpha(j_1) = c_\alpha(j_1, k_2)$, $t_{\bullet\circ}(j_1) = t$ and $t_{\circ\bullet}(j_1) = t(1 + e^{i(k_2 - 2\pi\phi j_1)})$. The spectrum of H without magnetic field is shown in Fig.7. There is characteristic zero energy states which are localized near zigzag and bearded boundaries[11].

One particle Schrodinger equation for each k_2 , $H_{cyl}(k_2)|E(k_2)\rangle = E(k_2)|E(k_2)\rangle$ by $|E\rangle = \sum_{j_1} (\psi_{\bullet}(j_1) c_{\bullet}^\dagger(j_1, k_2) + \psi_{\circ}(j_1) c_{\circ}^\dagger(j_1, k_2))|0\rangle$ is reformulated using a transfer matrix as ($\phi = p/q$, p and q are mutually prime.)

$$\begin{pmatrix} \psi_{\bullet}(q\ell + 1) \\ \psi_{\circ}(q\ell) \end{pmatrix} = M^\ell \begin{pmatrix} \psi_{\bullet}(1) \\ \psi_{\circ}(0) \end{pmatrix}$$

where M is a 2×2 matrix (see ?? for the precise definition). It implies that the boundary condition for zigzag-bearded boundaries is then $\psi_{\circ}(q\ell) = 0$ (bearded) and $\psi_{\circ}(0) = 0$ (zigzag).

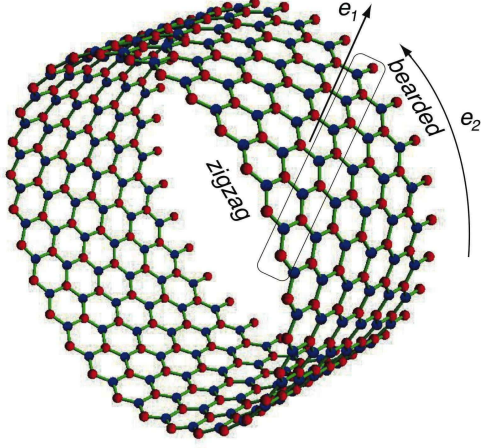


Figure 6. Graphene on a cylinder with zigzag and bearded edges. Unit cell of the dimensional system for the momentum representation by k_2 is shown.

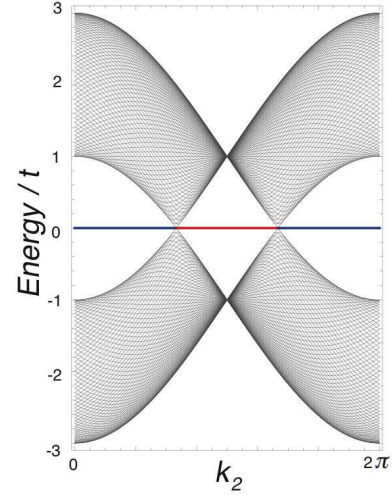


Figure 7. One particle energy spectrum of the graphene without magnetic field labelled by k_2 . There are zero mode boundary states. The red ones are localized at the zigzag boundary and the blue ones are localized at the bearded one[11, 35].

Then the spectrum $\epsilon_\ell(k_2)$ of the edge states is determined by $M_{21}(\epsilon_\ell) = 0$ and their position is specified as

$$\begin{aligned} \text{for zigzag-bearded: } |M_{11}(\epsilon_\ell)| &> 1 : \text{ right } j_1 \approx \infty : (\text{bearded edges}) \\ |M_{11}(\epsilon_\ell)| &< 1 : \text{ left } j_1 \approx 1 : (\text{zigzag edges}) \end{aligned}$$

When one consider the bearded-zigzag boundaries, the condition is $\psi_\bullet(q\ell + 1) = 0$ (zigzag) and $\psi_\bullet(1) = 0$ (bearded). Then the spectrum is determined by $M_{12}(\epsilon_\ell) = 0$ and

$$\begin{aligned} \text{for bearded-zigzag: } |M_{22}(\epsilon_\ell)| &> 1 : \text{ right } j_1 \approx \infty : (\text{zigzag edges}) \\ |M_{22}(\epsilon_\ell)| &< 1 : \text{ left } j_1 \approx 1 : (\text{bearded edges}) \end{aligned}$$

4.1. Zero mode boundary states

Graphene with zigzag edges without magnetic field has a characteristic boundary states (Fujita states) which has been also confirmed by a realistic first principle calculation and also experimentally[11, 36, 12]. By the general discussion above, we have ($\phi = 0$) the zero modes localized at the zigzag edge when $|M_{11}| = |1 + e^{ik_2}| < 1$ ($2\pi/3 < k_2 < 4\pi/3$) and at the bearded edge when $|M_{11}| = |1 + e^{ik_2}| > 1$ ($0 < k_2 < 2\pi/3, 4\pi/3 < k_2 < 2\pi$)[11, 35] as shown in Fig7. Actually the existence of the zero localize states is guaranteed by the bulk[35]. Let us first define the Berry phase (Zak phase) $\gamma(k_2)$ for each k_2 using a bulk hamiltonian $\mathbf{h}(\mathbf{k})$ as

$$\gamma_{Z,B}(k_2) = -i \int_0^{2\pi} dk_1 \psi_{Z,B}^\dagger \partial_{k_1} \psi_{Z,B} = 0 \text{ or } \pi \pmod{2\pi}$$

where $\psi_{Z,B}$ is an eigen state of the hamiltonian of the periodic systems $\mathbf{h}_{Z,B}$ (compatible with the zigzag or bearded edges. This quantization as Z_2 Berry phase is due to the chiral

symmetry[35, 29]. The zero modes which is compatible for the unit cell of the periodic system only exist when $\gamma(k_2) = \pi$.

$$\gamma_{Z,B}(k_2) = \begin{cases} \pi \pmod{2\pi} & : \text{zero modes exist at the zigzag (bearded) edges for } k_2 \\ 0 \pmod{2\pi} & : \text{no reason to have the zero mode for } k_2 \end{cases}$$

The condition for the zigzag boundary states, $|M_{11}| = |1 + e^{-ik_2}| < 1$, is the condition for the $\Delta_Z(\mathbf{k}) = 1 + e^{-ik_2} + e^{-ik_1}$ encloses the origin by changing $k_1 \rightarrow 2\pi$. Since the curve is a unit circle centered at $1 + e^{-ik_2}$, the distance between the origin and center $|1 + e^{-ik_2}|$ needs to be less than unity for the origin to be enclosed. *It establishes a bulk-edge correspondence of the zero mode boundary states for the zigzag edges.*

With a magnetic field, there still exist zero mode boundary states though the $n = 0$ Landau level also co-exists. Even though the bulk and the edge are both at the same energy, the local density of state at $E = 0$ shows characteristic behavior which is consistent with the localized boundary modes[37].

4.2. Quantum Hall edge states of Dirac fermions

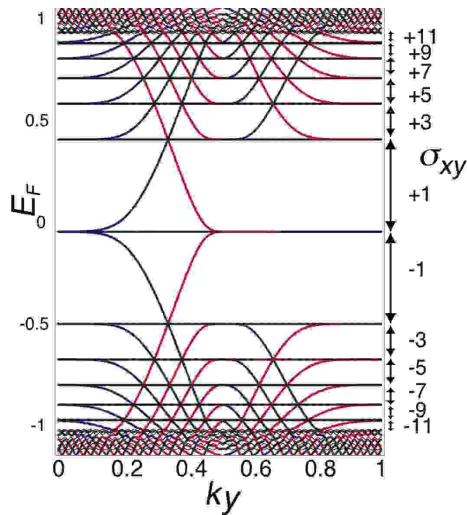


Figure 8. One particle energy spectrum of the graphene on a cylinder. The blue (red) lines are edge states localized near the left (right) edges. k_y is a momentum along the edges and the σ_{xy} 's when the fermi energy sit there are shown in unit $-e^2/h$. The numbers are the Chern numbers of the bulk and, at the same time, numbers of the blue (red) lines in the gap ($\phi = 1/51$). (See also [2])

Anomalous quantum Hall effect of graphene as of the Dirac fermions is also discussed with the boundaries on the cylindrical geometry. Then counting the light and left edges modes between the energy gap where the fermi energy lies, one can assign the Hall conductance using the Laughlin argument. Using the transfer matrix formulation given before, we can assign a winding number of the edge state on the complex energy surface, which is, in our case, a Riemann surface of genus g where g is a number of energy gaps (Landau gaps). Using the setup, one may prove a direct relation between the two topological numbers, the one is the Chern number and the other is a winding number of the edge state [38, 6, 16]. It reads physically

$$\sigma_{xy}^{\text{bulk}} = \sigma_{xy}^{\text{edge}}.$$

That is, the Hall conductance described by the bulk and the edges are the same. It should be like this. This is the bulk-edge correspondence of the Dirac fermions in graphene. In Fig.8, energy spectrum with the zigzag-bearded boundaries are shown as a function of k_2 and the corresponding Hall conductance. It confirms the principle.

Acknowledgement

We thank discussion with H. Aoki, T. Kawarabayashi, T. Fukui, M. Arai, T. Morimoto and H. Watanabe. The work is supported in part by Grants-in-Aid for Scientific Research, No.203400984 from JSPS and No.22014002 (Novel States of Matter Induced by Frustration) on Priority Areas from MEXT (JAPAN).

Appendix A. Landau Level with anisotropic mass

Let us summarize the standard Landau quantization of electrons with parabolic dispersion with (effective) anisotropic mass described by the following hamiltonian $H = \boldsymbol{\pi}^\dagger \frac{1}{2m} \boldsymbol{\Xi}_L \boldsymbol{\pi}$, ($\text{rot } \mathbf{A} = B\hat{z}$) where $\boldsymbol{\pi} = \begin{pmatrix} \pi_x \\ \pi_y \end{pmatrix}$, $\pi_i = p_i - eA_i = \pi_i^\dagger$ and $\boldsymbol{\Xi}_L = \begin{pmatrix} \xi_x & \xi_{xy} \\ \xi_{xy} & \xi_y \end{pmatrix}$ is a real symmetric anisotropy matrix. It satisfies $[\pi_x(\ell_B/\hbar), \pi_y(\ell_B/\hbar)] = i$ ($\ell_B = \sqrt{\frac{\hbar}{eB}}$). Since the matrix $\boldsymbol{\Xi}_L$ is real symmetric, it is diagonalized by the orthogonal matrix as $\boldsymbol{\Xi}_L = \mathbf{V}^\dagger \boldsymbol{\Xi}_D \mathbf{V} = \mathbf{V}^\dagger \boldsymbol{\Xi}_D \mathbf{V}$ $\boldsymbol{\Xi}_D = \text{diag}(\xi_X, \xi_Y)$, $\xi_X \xi_Y = \det \boldsymbol{\Xi}_L$, $\xi_X + \xi_Y = \text{Tr } \boldsymbol{\Xi}_L$. $\mathbf{V} = \begin{pmatrix} \cos \theta & -\sin \theta \\ \sin \theta & \cos \theta \end{pmatrix}$, $\exists \theta \in \mathbb{R}$. Then we have $H = \boldsymbol{\Pi}^\dagger \boldsymbol{\Xi}_D \boldsymbol{\Pi}$, $\boldsymbol{\Pi} \equiv \mathbf{V} \boldsymbol{\pi}$, $[\Pi_X(\ell_B/\hbar), \Pi_Y(\ell_B/\hbar)] = i$.

Now defining a bosonic operator, ($[a, a^\dagger] = 1$) $a = (\ell_B/\hbar)(\Pi_X + i\Pi_Y)/\sqrt{2}$, the hamiltonian is written as $H = \frac{\hbar\omega}{4} \left(\xi_X (a + a^\dagger)^2 - \xi_Y (a - a^\dagger)^2 \right)$ where $\omega = \frac{eB}{m}$ is a cyclotron frequency.

Now we define a new bosonic operator ($[b, b^\dagger] = 1$) as $a = ub + v^*b^\dagger$ requiring $[a, a^\dagger] = [ub + v^*b^\dagger, u^*b + vb] = |u|^2 - |v|^2 = 1$. Here noting that $\xi_X (a + a^\dagger)^2 - \xi_Y (a - a^\dagger)^2 = b^2 \{ \xi_X (u + v)^2 - \xi_Y (u - v)^2 \} + h.c. + (bb^\dagger + b^\dagger b) \{ \xi_X |u + v|^2 + \xi_Y |u - v|^2 \}$, we choose as $\xi_X (u + v)^2 = \xi_Y (u - v)^2$, $u + v = C\sqrt{\xi_Y}$, $u - v = \pm C\sqrt{\xi_X}$. Assuming $\xi_X, \xi_Y > 0$ and imposing $|u|^2 - |v|^2 = 1$, we have $|C|^2 = 1/\sqrt{\xi_X \xi_Y} = 1/(\det \boldsymbol{\Xi}_L)^{1/2}$, $u = \frac{\sqrt{\xi_X + \sqrt{\xi_X \xi_Y}}}{2(\det \boldsymbol{\Xi}_L)^{1/4}}$, $v = \frac{-\sqrt{\xi_X + \sqrt{\xi_X \xi_Y}}}{2(\det \boldsymbol{\Xi}_L)^{1/4}}$.

Finally the hamiltonian is written as

$$H = \frac{1}{2} \hbar\omega (bb^\dagger + b^\dagger b) |C|^2 (\xi_X \xi_Y) = \hbar\omega_\Xi (b^\dagger b + \frac{1}{2})$$

where $\omega_\Xi = \omega \sqrt{\det \boldsymbol{\Xi}_L} = \frac{eB}{m} \sqrt{\xi_X \xi_Y}$. As for the Landau degeneracy, we stressed that it is independent of the anisotropy since the magnetic length is independent of the mass.

Appendix B. Some notations of differential form

In this appendix, we supplement some details for the differential forms which may not be so popular as the standard vector analysis.

- We have omitted the wedge product (\wedge) which is anti-commuting and useful for the integral over the oriented surface. For example, $d\phi^1 \wedge d\phi^2 = -d\phi^2 \wedge d\phi^1$ and $d\phi^1 \wedge d\phi^1 = -d\phi^1 \wedge d\phi^1 = 0$. It implies

$$\langle dG | dG \rangle \equiv \langle dG | \wedge | dG \rangle = d\phi^\mu \langle \partial_\mu G | \wedge d\phi^\nu | \partial_\nu G \rangle = d\phi^1 \wedge d\phi^2 [\langle \partial_1 G | \partial_2 G \rangle - \langle \partial_2 G | \partial_1 G \rangle]$$

- For any (matrix valued) one form $\mathbf{X} = \mathbf{X}_\mu d\phi^\mu$, $\text{Tr } \mathbf{X}^2 = 0$

$$\text{Tr } \mathbf{X}^2 = \text{Tr } \mathbf{X}_\mu \mathbf{X}_\nu d\phi^\mu d\phi^\nu = \text{Tr } \mathbf{X}_\nu \mathbf{X}_\mu d\phi^\mu d\phi^\nu = \text{Tr } \mathbf{X}_\mu \mathbf{X}_\nu (-d\phi^\nu d\phi^\mu) = -\text{Tr } \mathbf{X}^2$$

- As for a matrix valued function $\boldsymbol{\omega}$, $d\boldsymbol{\omega}^{-1} = -\boldsymbol{\omega}^{-1} d\boldsymbol{\omega} \boldsymbol{\omega}^{-1}$. It obeys from $0 = d\mathbf{E} = d(\boldsymbol{\omega} \boldsymbol{\omega}^{-1}) = (d\boldsymbol{\omega}) \boldsymbol{\omega}^{-1} + \boldsymbol{\omega} d\boldsymbol{\omega}^{-1}$.

- Gauge transformation of the non-Abelian gauge strength $F_M = dA_M + A_M^2$ where $A_M = \omega^{-1}A'_M\omega + \omega^{-1}d\omega$.

$$\begin{aligned}
F_M &= d(\omega^{-1}A'_M\omega) + d(\omega^{-1}d\omega) + \omega^{-1}A_M^2\omega + \omega^{-1}A'_Md\omega + \omega^{-1}d\omega\omega^{-1}A'_M\omega + (\omega^{-1}d\omega)^2 \\
&= -\omega^{-1}d\omega\omega^{-1}A'_M\omega + \omega^{-1}dA'_M\omega - \omega^{-1}A'_Md\omega - \omega^{-1}d\omega\omega^{-1}d\omega \\
&\quad + \omega^{-1}A_M^2\omega + \omega^{-1}A'_Md\omega + \omega^{-1}d\omega\omega^{-1}A'_M\omega + (\omega^{-1}d\omega)^2 = \omega^{-1}F'_M\omega
\end{aligned}$$

References

- [1] Wallace P R 1947 *Phys. Rev.* **71** 622
- [2] Lomer W H 1955 *Proc. Roy. Soc. (London)* **A227** 330
- [3] McClure J W 1956 *Phys. Rev.* **104** 666
- [4] Novoselov K S, Geim A K, Morozov S V, Jiang D, Katsnelson M I, Grigorieva I V, Dubonos S V and Firsov A A 2005 *Nature* **438** 197
- [5] Zhang Y, Tan Y, Stormer H and Kim P 2005 *Nature* **438** 201
- [6] Hatsugai Y 1993 *Phys. Rev. Lett.* **71** 3697
- [7] Qi X L and Zhang S C 2010 *Physcs today* **63** 33
- [8] Moore J E 2010 *Nature* **464** 194
- [9] Hasan M Z and Kane C L *arXiv:1002.3895*
- [10] Wang Z, Chong Y, Joannopoulos J D and Soljacic M 2009 *Nature* **461** 772
- [11] Fujita M, Wakabayashi K, Nakada K and Kusakabe K 1996 *J. Phys. Soc. Jpn.* **65** 1920
- [12] Kobayashi Y, Fukui K, Enoki T, Kusakabe K and Kaburagi Y 2005 *Phys. Rev. B* **71** 193406
- [13] Nielsen H B and Ninomiya M 1981 *Nucl. Phys. B* **185** 20
- [14] Zheng Y and Ando T 2005 *Phys. Rev. B* **65** 245420
- [15] Gusynin V P and Sharapov S 2005 *Phys. Rev. Lett.* **95** 146801
- [16] Hatsugai Y, Fukui T and Aoki H 2006 *Phys. Rev. B* **74** 205414
- [17] Guinea F, Horovitz B, and Doussal P L 2008 *Phys. Rev. B* **77** 205421
- [18] Kawarabayashi T, Hatsugai Y and Aoki H 2009 *Phys. Rev. Lett.* **103** 156804
- [19] Hatsugai Y, Fukui T and Aoki H 2007 *Eur. Phys. J. Special topics* **148** 133
- [20] Hatsugai Y 2010 *New J. Phys.* **12** 065004
- [21] Creutz M 2008 *JHEP* **04** 017
- [22] Aharonov Y and Casher A 1979 *Phys. Rev. B* **19** 2461
- [23] Niu, Thouless D J, and Wu Y S 1985 *Phys. Rev. B* **31** 3372
- [24] Berry M V 1984 *Proc. R. Soc.* **A392** 45
- [25] Flanders H 1989 *Differential Forms with Applications to the Physical Sciences* (Dover Publ.)
- [26] Kohmoto M 1985 *Ann. Phys. (N. Y.)* **160** 355
- [27] Hatsugai Y 2004 *J. Phys. Soc. Jpn.* **73** 2604
- [28] Hatsugai Y, Ryu S and Kohmoto M 2004 *Phys. Rev. B* **70** 054502
- [29] Hatsugai Y 2006 *J. Phys. Soc. Jpn.* **75** 123601
- [30] Hatsugai Y 2005 *J. Phys. Soc. Jpn.* **74** 1374
- [31] Wilczek F and Zee A 1984 *Phys. Rev. Lett.* **52** 2111
- [32] Thouless D J, Kohmoto M, Nightingale P and den Nijs M 1982 *Phys. Rev. Lett.* **49** 405
- [33] Fukui T, Hatsugai Y and Suzuki H 2005 *J. Phys. Soc. Jpn.* **74** 1674
- [34] Arai M and Hatsugai Y 2009 *Phys. Rev. B* **79** 075429
- [35] Ryu S and Hatsugai Y 2002 *Phys. Rev. Lett.* **89** 077002
- [36] Okada S and Oshiyama A 2001 *Phys. Rev. Lett.* **87** 146803
- [37] M Arikawa Y H and Aoki H 2008 *Phys. Rev. B* **78** 205401
- [38] Hatsugai Y 1993 *Phys. Rev. B* **48** 11851